

Self-Sorting of Four Organic Molecules into a Heterowheel Polypseudorotaxane

Liang Li,^[a, b] Heng-Yi Zhang,^[a] Jin Zhao,^[a] Nan Li,^[a] and Yu Liu^{*[a]}

Abstract: The social self-sorting supramolecular assembly is described by non-covalent interactions among four organic components. Toward this goal, a series of self-sorting systems have been investigated by mixing two or three different compounds; naphthyl-bridged bis(α -cyclodextrin), *N,N'*-dioctyl-4,4'-bipyridinium, 2,6-dihydroxynaphthalene, and cucurbit[8]uril. The influence of alkyl chains of viologen derivatives and the binding abilities of

these systems have also been studied. Their integrative self-sorting led to the exclusive formation of the purple supramolecular heterowheel polypseudorotaxane. The heterowheel polypseudorotaxane is a thermodynamically stable self-sorted product, and consists

Keywords: cyclodextrins • host–guest chemistry • rotaxanes • self-assembly • supramolecular chemistry

of two different macrocycles with three sorts of different non-covalent interactions. Its structure was established by NMR spectroscopy and UV/Vis absorption spectroscopy, transmission electron microscopy (TEM), atomic force microscopy (AFM), dynamic light-scattering (DLS), diffusion-ordered spectroscopy (DOSY), and viscosity measurements.

Introduction


It is well-known that DNA replication begins at specific locations in the genome, in which the four organic nucleic acid bases matched to the template strand to generate the new DNA double strand in the presence of DNA polymerase. The almost perfect fidelity recognition among these nucleic acid bases can be referred to as social self-sorting.^[1] To date, the artificial social self-sorting systems were mainly constructed from two components^[2–5] and three components.^[6–11] In all reported multicomponent (over three) artificial social self-sorting systems,^[12] the metal ion is always an essential component and the metal-coordination bonds are one of the most important forces. However, compared with other non-covalent interactions, the stronger bonding-energy of metal ions with ligands and the resultant poorer reversibility become a disadvantage for constructing artificial social self-sorting biologic systems. Thus, the design of

functional molecular building blocks for simulating complicated biological systems remains challenging.

Cyclodextrins (CDs) have been extensively studied as not only excellent water soluble receptors for molecular recognition but also convenient building blocks to construct nanostructured supramolecular architectures by hydrophobic interactions,^[13] whereas cucurbiturils (CBs) can form stable host–guest complexes with positively charged molecules by charge-transfer (CT) interactions.^[14] In this respect, cucurbit[8]uril (CB[8]) is a useful molecular connector.^[15] Its 1:1:1 ternary complex with the positively charged viologen and electron-rich naphthoxy derivatives is a powerful and effective platform for elongating polymer chains,^[16] immobilizing colloids onto the Au substrates^[17] and preparing network,^[18] protein-polymer conjugation,^[19] and heterowheel [3]pseudorotaxane.^[20] Hence, the combination of CDs and CBs becomes an important topic for designing functional supramolecular assemblies.^[21] Herein, we firstly report a fully organic four-component social self-sorting supramolecular assembly. This supramolecular assembly can be exclusively obtained through randomly mixing naphthyl-bridged bis(α -CD) (**1**), *N,N'*-dioctyl-4,4'-bipyridinium (**2**), CB[8], and 2,6-dihydroxynaphthalene (**3**). By using transmission electron microscopy (TEM), atomic force microscopy (AFM), dynamic light-scattering (DLS), diffusion-ordered spectroscopy (DOSY) and viscosity measurements, we will demonstrate that the social self-sorting supramolecular assembly results in a heterowheel polypseudorotaxane by the non-covalent interactions of hydrophobic, ion-dipole and charge-transfer interactions.

[a] Dr. L. Li, Dr. H.-Y. Zhang, J. Zhao, N. Li, Prof. Dr. Y. Liu
Department of Chemistry
State Key Laboratory of
Elemento-Organic Chemistry
Nankai University, Tianjin
300071 (P.R. China)
Fax: (+86) 22-2350-3625
E-mail: yuliu@nankai.edu.cn

[b] Dr. L. Li
School of Chemical and
Environmental Engineering
Shanghai Institute of Technology
Shanghai, 201418 (P.R. China)

 Supporting information for this article (including materials, methods and characterization techniques) is available on the WWW under <http://dx.doi.org/10.1002/chem.201204583>.

Results and Discussion

Preparation of compound 1: Compound **1** was prepared by the copper-catalyzed triazole click reaction of 6-deoxy-6-azide- α -CD with 1,5-bis(prop-2-ynyloxy)naphthalene (Np), following the typical procedure as previously reported (Figure 1).^[22] To ascertain the conformation of **1**, we firstly carried out NMR experiments of **1** in D₂O. In its 2D NOESY spectrum (see the Supporting Information, Figure S2), no NOE correlations between the Np moiety and inner protons of CD were observed, indicating that the Np moiety must not be in the cavity of α -CD.

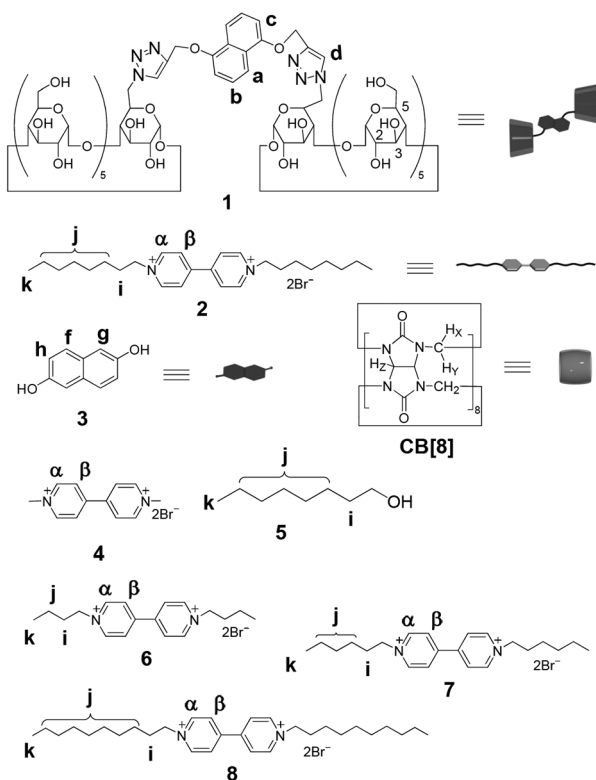
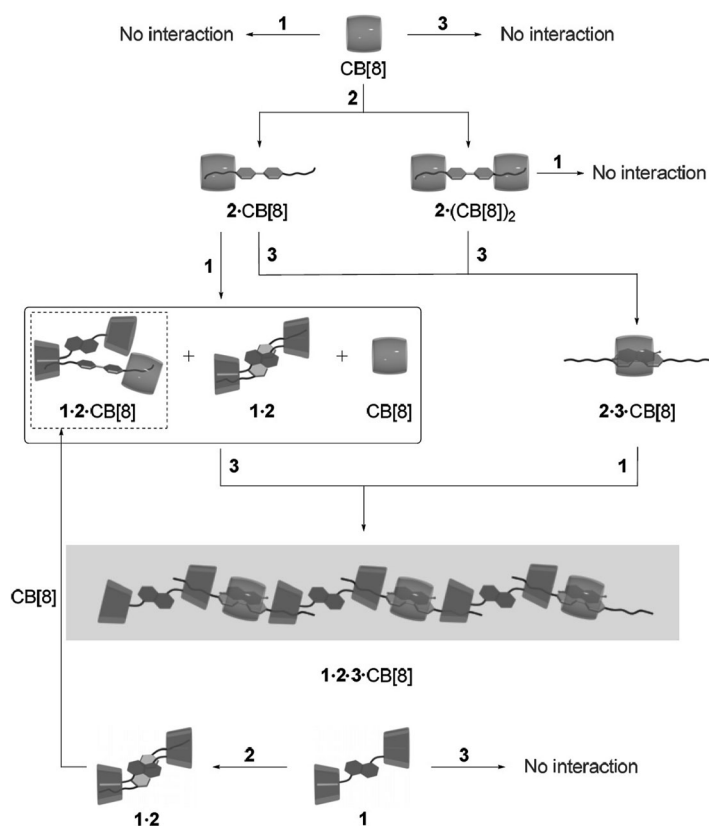


Figure 1. Structure of compounds **1–8** and CB[8].

Formation of polypseudorotaxane from 1: Compound **1** and CB[8] are two different category host molecules, so they can recognize different types of guests. To understand the self-sorting process of the four-component polypseudorotaxane, we selected respectively **1** and CB[8] as starting materials to investigate the self-sorting system (Scheme 1). Firstly, we selected **1** as the starting material. When CB[8] was added to the aqueous solution of **1**, no interaction was observed. However, when CB[8] was replaced with **2**, the complexation between **1** and **2** can be monitored by using ¹H NMR spectroscopy and electrospray ionization mass spectrometry (ESI-MS) experiments. As shown in Figure 2D, the signals for H_a, H_b, H_c of **1**, and H_β of **2** all shift upfield by $\delta = 0.76$, 0.22, 0.46, and 0.62 ppm, respectively, whereas H_d of **1** and the aliphatic protons (H_j and H_k) of **2** are shifted downfield



Scheme 1. Formation of the heterowheel polypseudorotaxane through a social self-sorting strategy of four organic components **1–3** and CB[8].

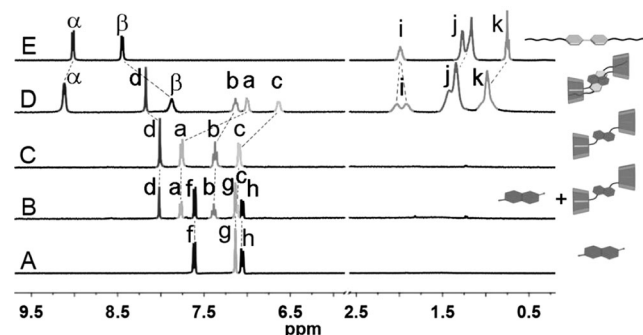


Figure 2. ¹H NMR (400 MHz, D₂O) spectra of A) **3** (2.0 mM), B) **1** (1.85 mM) + **3** (1.90 mM), C) **1** (2.0 mM), D) **1** (1.85 mM) + **2** (1.85 mM), E) **2** (2.0 mM).

by $\delta = 0.13$, 0.19, and 0.24 ppm, respectively. These observations indicate the formation of complex of **1** with **2**. In its 2D ROESY spectrum, the cross-peaks between H_a and H_b of **1** and H_β of **2** clearly suggest that the Np moiety and bipyridinium are located directly over each other. Therefore, it is reasonable that there is a 1:1 intermolecular charge-transfer complex. On the other hand, the correlations between aliphatic protons (H_j and H_k) and the inner protons of CDs demonstrate that the octyl chains insert into the cavity of α -CD from the primary face (see the Supporting Information, Figure S4, and Figure 7a). In the presence of

2.5 equivolar **2**, the chemical signals of all the protons are almost unchanged (see the Supporting Information, Figure S5). The strong binding affinity and 1:1 stoichiometry of **1**·**2** are further confirmed by the ESI mass spectrum, in which only one peak at m/z 1307.0 (attributed to $[\mathbf{1}\cdot\mathbf{2}-2\text{Br}]^{2+}$) was observed (the Supporting Information, Figure S6). In the aqueous solution, there are two pairs of induced circular dichroism (ICD) signals upon the addition of one equivolar **2** into the solution of **1**. On the basis of Kajita's rule,^[23] the weak positive Cotton effect peak at 320 nm, and the strong negative Cotton effect peaks at 228 and 287 nm reveal that Np in **1** locates out of the primary side of CD moiety and parallels the axes of two CDs, whereas the weak positive peak at 260 nm suggests that the octyl moiety should be included in the cavity of α -CD. Meanwhile, the electric transition polarized along the long axis of bipyridinium group is perpendicular to the axis of CDs (see the Supporting Information, Figure S7). When equivolar **3** was added into the solution of **1**, the resonances of its aromatic protons hardly changed. Moreover, the 2D ROESY of **1** in the presence of **3** exhibits that there are no correlations between the naphthyl protons of **3** and the inner protons of the cavity of CD in **1**. These observations indicate that there is no interaction between **1** and **3** (Figure 2B and the Supporting Information, Figure S8).

We carried out the NMR experiments to investigate the influence of CB[8] or **3** on the robust divalent complex **1**·**2**. In the NMR spectrum of **1**·**2** in the presence of equivolar CB[8] (Figure 3C), the proton signals of **2** in complex **1**·**2**

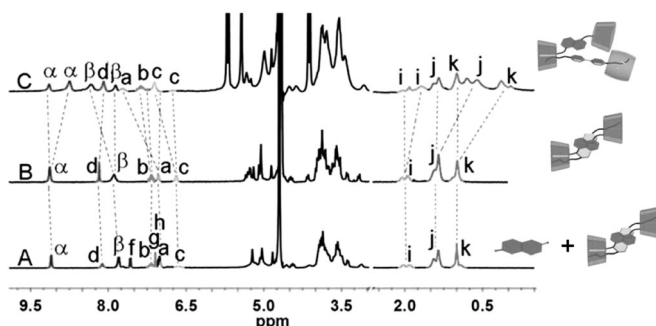


Figure 3. ¹H NMR (400 MHz, D₂O) spectra of A) **1**·**2** (1.85 mM) + **3** (1.90 mM), B) **1** (1.85 mM) + **2** (1.85 mM), C) **1**·**2** (1.85 mM) + CB[8] (1.90 mM) at 298 K.

divide into two parts, indicating that there are more than one species with a slow exchange rate on the ¹H NMR time-scale. Meanwhile, the upfield shift of aliphatic protons suggests that the methyl group is included deeply in the cavity of CB[8]. These observations indicate that one octyl group of **2** is encapsulated into the cavity of CB[8]. Furthermore, the NOE correlations between H₅ of **1** and H_j of **2** as well as between H₃ of **1** and H_x of CB[8] provide strong evidence for one CD encapsulating one octyl group of **2** from the primary face, and the other CD and CB[8] being closed in the ternary complex **1**·**2**·CB[8] (see the Supporting Information,

Figure S9). The ESI-MS measurement also validates the above results. The peaks of 1307.0 and 1971.7 are attributed to $[\mathbf{1}\cdot\mathbf{2}-2\text{Br}]^{2+}$ and $[\mathbf{1}\cdot\mathbf{2}\cdot\text{CB}[8]-2\text{Br}]^{2+}$, respectively (Figure 4). Upon addition of 2.0 equivolar CB[8], the

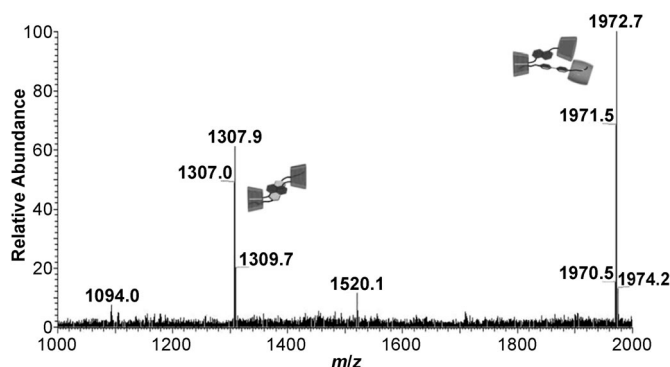


Figure 4. Partial ESI-MS spectrum of a solution containing complex **1**·**2** (1.0 equiv), and CB[8] (1.0 equiv) in water. The full spectrum can be found in Figure S10 in the Supporting Information

proton signals of **1** return to its origin location, whereas the signals of the octyl moiety in **2** further shifts to higher field, and H_β on bipyridinium shifts downfield, which indicates that the other octyl chains encapsulate into the cavity of CB[8]. The broader peaks in experiment B compared with those in C should be attributed to compound **2** quickly exchanging between the formation of complex **2**·(CB[8])₂ and the dissociation of complex **1**·**2**·CB[8] at the NMR timescale (see the Supporting Information, Figure S11). In the ICD spectra of a titration of CB[8] into the solution of complex **1**·**2**, both positive and negative ICD signals gradually decrease to half upon addition of one equivolar CB[8]. This observation suggests that one octyl chain of **2** is moved from the cavity of CD and then is included in the cavity of CB[8], resulting in the formation of the ternary complex **1**·**2**·CB[8]. When CB[8] is increased to 2 equivolar, the ICD signals almost disappear (Figure 5), which indicates that all octyl chains of **2** are outside cavity of CD. On the other hand, the addition of equivolar **3** to the solution of **1**·**2** does not change the chemical shifts of the protons (Figure 3A), which demonstrates that there is no interaction between the complex **1**·**2** and **3**, consistent with the illustration shown in Figure 2B.

Although compound **3** interacts with neither **1** nor complex **1**·**2**, we wanted to reveal its influence on complex **1**·**2**·CB[8]. As shown in Figure 6B, the proton signals of naphthyl group in **1** are similar to that of free **1**, H_i, H_j, H_k in **2** shift downfield, whereas H_α and H_β in **2** and H_f, H_g, and H_h in **3** shift upfield. These observations are indicative of two important parts: the encapsulation of the octyl moiety in the cavity of CDs and the complexation of **2** with **3** inside the cavity of CB[8]. Furthermore, NOE correlations between the octyl group (H_j, H_k) of **2** and H₅ of α -CD in **1**, as well as H_x and H_z of CB[8] and H₂ of α -CD in **1** provide strong evidence for not only α -CD penetrating into the octyl

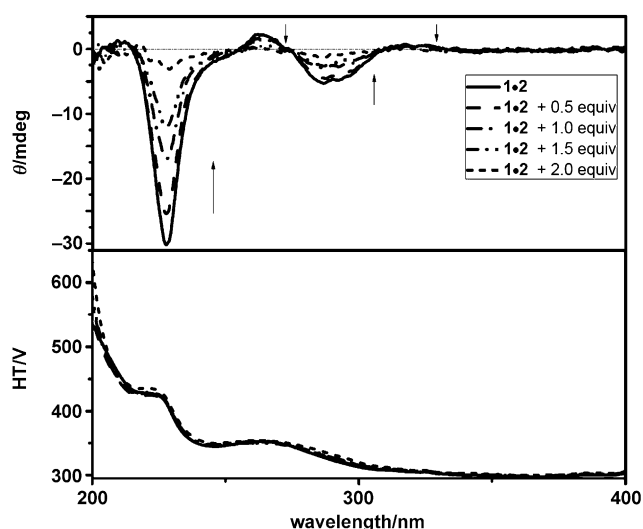


Figure 5. Circular dichroism spectra of a 1:1 mixture of **1** (0.12 mM) and **2** (0.12 mM) with the addition of CB[8] (0, 0.06, 0.12, 0.18, and 0.24 mM) in aqueous solution.

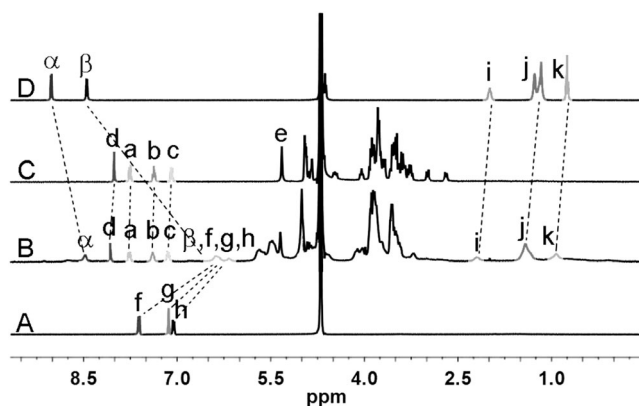


Figure 6. ^1H NMR (400 MHz, D_2O) spectra of A) **3**, B) **1•2•CB[8]** (1.85 mM) + **3** (1.90 mM), C) **1** (2.0 mM), D) **2** (2.0 mM) at 298 K.

chain from its secondary side, but also the two macrocycles being closely located (see the Supporting Information, Figure S12, and Figure 7b). The combined results demonstrate the formation of polypseudorotaxane **1•2•3•CB[8]**, as illustrated in Scheme 1.

Formation of Polypseudorotaxane from CB[8]: ^1H NMR spectra were firstly performed between equimolar CB[8] and **2** in D_2O . As shown in Figure 8, the resonances of all protons in **2** shift upfield, accompanied by the splitting of the signal of H_j from double peaks to triple peaks. These observations reveal that CB[8] remains in equilibrium between the bipyridinium nucleus and the octyl moieties of **2**. In the ESI-MS of **2** in the presence of CB[8] (see the Supporting Information, Figure S13), the strong peak at m/z 855.4 is attributed to $[\mathbf{2}\cdot\text{CB[8]}-2\text{Br}]^{2+}$, indicating the formation of complex **2•CB[8]**. In a control experiment, the addition of equimolar **3** into the solution of **2** hardly changes the chemi-

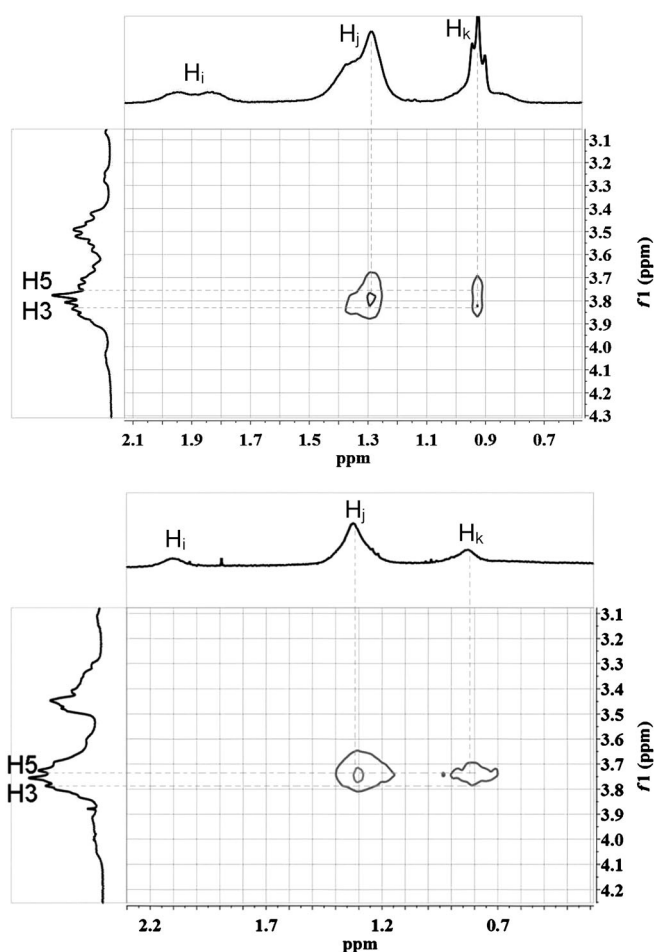


Figure 7. Partial ROESY spectra of a mixture of a) **1** (1.85 mM) + **2** (1.85 mM) and b) **1•2•CB[8]** (1.85 mM) + **3** (1.90 mM) in D_2O at 298 K. Their full spectra are shown in Figures S4 and S12 of the Supporting Information, respectively.

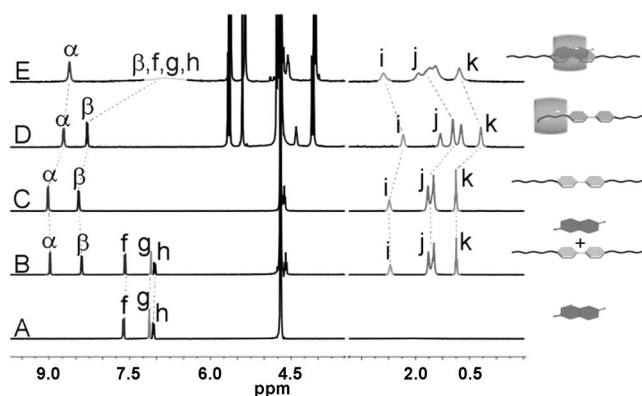


Figure 8. A) **3** (2.00 mM), B) **2** (1.85 mM) + **3** (2.00 mM), C) **2** (2.0 mM), D) **2** (1.85 mM) + CB[8] (1.90 mM), E) **2** (1.85 mM) + **3** (1.90 mM) + CB[8] (1.90 mM) at 298 K.

cal shifts of **2** (Figure 8B), which is in accordance with similar systems.^[24] In sharp contrast, when equimolar **3** was added into the solution of complex **2•CB[8]**, the H_α and H_β of **2** and the naphthyl protons of **3** shift to high fields, whereas the octyl moiety signals in **2** shift downfield (Figure 8E).

A similar result from the control experiment was also observed in NMR spectrum of complex **2**·(CB[8])₂ in the presence of **3** (the Supporting Information, Figure S14). These observations confirm the complexation of the bipyridium moiety in **2** with **3** in the cavity of CB[8]. As a result, the formation of the stable CT complex **2**·**3**·CB[8], like the ternary complex (**3**·methyl viologen·CB[8]), is a natural process. The signal in the ESI-MS at *m/z* 935.9 is assigned to [**2**·**3**·CB[8]–2Br[–]]²⁺ (the Supporting Information, Figure S15), which also proves the formation of the ternary **2**·**3**·CB[8] complex.

When **1** was added into the solution of complex **2**·**3**·CB[8], the signals of the octyl-group protons (H_i, H_j, and H_k) in **2** exhibit an upfield shift in the NMR spectrum, which indicates that the octyl chains must be inserted into the cavity of the CD of **1** (the Supporting Information, Figure S16 A). A similar phenomenon is also found in the following control experiment. As shown in Figure S16 B (the Supporting Information), the addition of α-CD into the solution of **2**·**3**·CB[8] shows that H_α and H_β of **2** and H_f, H_g, and H_h of **3** shift to high fields, whereas H_i, H_j, and H_k shift downfield. These observations suggest that α-CD also binds the octyl moiety of **2** from the secondary face,^[25] leading to the formation of pseudorotaxane α-CD·**2**·**3**·CB[8].

Formation of polypseudorotaxane in one pot: On the basis of above analyses, we believed that the polypseudorotaxane may also be obtained by mixing the four components in one pot. Firstly, the ¹H NMR spectrum of the mixture of **1**, **2**, **3**, and CB[8] is the same as that of the above step-combinations, which suggests that this social self-sorting process occurs in this system (Supporting Information, Figure S17).

In the controlled experiments, when mixing the five components (**3**, **4**, **5**, α-CD and CB[8]) in one pot, the signals of the bipyridium protons in **4** and the naphthyl group in **3** exhibit a upfield shift, and those of the octyl group in **5** shift downfield in the NMR spectrum, which indicates that the pyridium moiety and **3** forms a stable complex with CB[8] and the octyl chains insert into the cavity of the α-CD (the Supporting Information, Figure S18). The above results demonstrate that a mixture of the five components forms two stable complexes, which experience the social self-sorting process. These observations confirm the formation of a polypseudorotaxane between **1**, **2**, **3**, and CB[8].

To further understand the role of CB[8] and CDs in the process of controlling the binding behavior, we performed UV/Vis absorption experiments on this system. Upon addition of equimolar **2** to the solution of **1**, a new absorption band is observed (centered at 475 nm), which is assigned to the CT interaction between **1** and **2**. When CB[8] was added to the above solution, the absorption band at 475 nm decreased. This observation suggests the disassociation of the complex **1**·**2** and the formation of the ternary complex **1**·**2**·CB[8]. When continuing to add **3**, a new absorption band at 560 nm was observed, which is attributed to the formation of the more-stable CT complex **2**·**3**·CB[8], accompanied with the dissociation of the ternary complex **1**·**2**·CB[8]

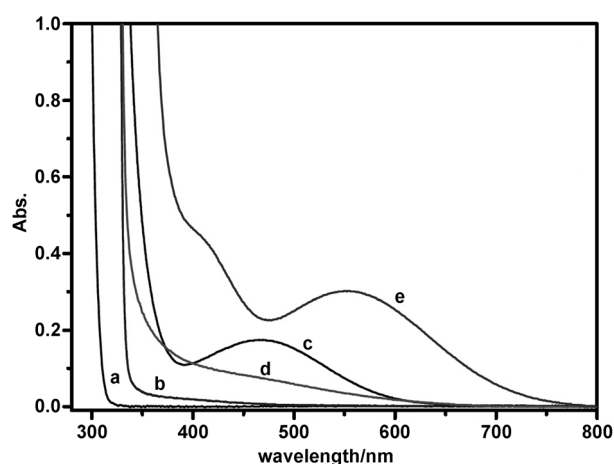


Figure 9. UV/Vis spectra in aqueous of a) **1** (1.0 mM), b) **2** (1.0 mM), c) mixture of **1** (1.0 mM) and **2** (1.0 mM), d) mixture of **1**·**2** (1.0 mM) and CB[8] (1.0 mM), e) mixture of **1**·**2**·CB[8] (1.0 mM) and **3** (1.0 mM).

(Figure 9). These combined observations suggest that the social self-sorting process is thermodynamically controlled, and depends mainly on the difference from the molecular recognition capacity of CB[8] and CDs.

The influence of the alkyl chains: To obtain further insight into the role of alkyl chains in viologens, we synthesized additional three viologen derivatives with different alkyl-chain lengths (Figure 1); namely, *N,N'*-dibutyl-4,4'-bipyridinium (**6**), *N,N'*-dihexyl-4,4'-bipyridinium (**7**), and *N,N'*-didecyl-4,4'-bipyridinium (**8**), respectively. With the exception of viologens with shorter aliphatic *N*-substituents (*n* ≤ 3), compounds **2**, **6**–**8** or other viologens with longer aliphatic *N*-substituents favor the formation of complex with **1**.^[25,26] Upon addition of these viologen derivatives to the solution of **1**, the color of their solutions change from colorless to light-red, accompanied by the appearance of a new absorption band at 475 nm. However, the intensity of the absorption band at 475 nm is different for the four complexes; complex **1**·**6** is the strongest, and **1**·**8** is the weakest. The appearance of the new absorption band should be attributed to CT interactions between the Np moiety of **1** and bipyridinium of viologen derivatives, whereas the difference of their strength is perhaps due to the stronger hydrophobic interaction between the longer alkyl chains and the cavity of CD (see the Supporting Information, Figure S19). Whereas, upon increasing the length of the alkyl chains of viologen derivatives, the absorption band strength at 560 nm is decreased from **6**, **7**, **2** to **8**, which is due to the steric hindrance of the longer alkyl chains (see the Supporting Information, Figure S20). These observations suggest that increasing the chain length of viologens can affect the formation of ternary complex of viologens, **3**, and CB[8].

When **1**, **3**, CB[8] and one of viologen derivatives (**6**, **7**, **2**, **8**) were mixed in D₂O solutions, the NMR experiments were performed in turn. The signals of alkyl protons (H_i, H_j, H_k) in **6** hardly change and these chemical shifts are similar

to those of mixture of **3**, **6** with CB[8] (the Supporting Information, Figure S21). Although the proton signals of alkyl chains in **8** exhibit a minor downfield chemical shift (the Supporting Information, Figure S22), they are similar to the chemical shifts of the mixture of **1** with **8**. These observations indicate that there is no heterowheel polypseudorotaxane in the two cases. Whereas the protons (H_i , H_j , and H_k) of **2** and **7** give downfield shifts of $\delta=0.12$, 0.19, 0.20 ppm and 0.09, 0.07, 0.06 ppm, respectively (see Supporting Information, Figures S23 and S24), this observation indicates that the longer chains of **2** can build higher-degree polymerization supramolecular assemblies than that of **7** because of the stronger hydrophobic interaction between alkyl chains and the cavity of CD. All these considerations led us to a conclusion that **2** is a best choice in this self-sorting system.

Binding constant and molecular recognition of CB[8] and **1**:

To investigate quantitatively the molecular binding behavior of these four components and their thermodynamic control factors, the isothermal titration calorimetry (ITC) experiments were performed in phosphate buffers (pH 7.2).

As can be seen from Figure 10, the stoichiometries of complexation (n value) obtained from the curve fitting of the binding isotherm is close to 1, indicating that the formation of the 1:1 complex between **1** and **2**. Meanwhile, the complexation process is driven by favorable enthalpy changes ($\Delta H^\circ = -66.0 \text{ kJ mol}^{-1}$), accompanied by the negative entropy changes ($T\Delta S^\circ = -6.95 \text{ kJ mol}^{-1}$).

For the complexation of **2** with CB[8], the calorimetric titration curve does not fit the simple 1:1 model, and the simultaneous or stepwise 1:2 binding model also failed to fit to these experimental data. Carefully observing the titration curve under the ratio of **2** and CB[8] between 0 and 1, it is easy to find that there are two complexation processes (see the Supporting Information, Figure S25). Moreover, NMR titrations of **2** into the CB[8] solution also yield the 1:1 complex and the 1:2 complex with two inflection points at the ratio of 0.5 and 1.0, respectively. The **2**/CB[8] ratio is from 0.5 to 1.0, suggesting that both the 1:1 **2**-CB[8] complex and 1:2 **2**-(CB[8])₂ complex exist (see Supporting Information, Figures S26 and S27). Thus, its binding constant cannot be calculated exactly by using ITC. However, its enthalpy change (ΔH°) value, measured by using Equation (4) (in the Supporting Information), is $-24.5 \text{ kJ mol}^{-1}$. The favorable enthalpy change is likely attributed to the van der Waals interaction between the aliphatic chain and the inner wall of the host cavity.

Analysis of the enthalpy and entropy values in Table 1 reveals that the formation of complexes **1**·**2** and **2**-CB[8] are enthalpically driven. We reported that the intermolecular complexation of α -CD and **2** is driven by favorable enthalpy.^[25] As can be seen in Table 1, the K_s value ($3.3 \times 10^6 \text{ M}^{-1}$) of complex **1**·**2** is three orders of magnitude larger than that of α -CD with **2**, owing to the pre-organization between the naphthyl of **1** and bipyridium of **2** and the cavity of CD **1** and octyl chains of **2**. The K_s value ($1.4 \times 10^5 \text{ M}^{-1}$) of CB[8] and **2** determined by UV/Vis spectra (see Supporting Infor-

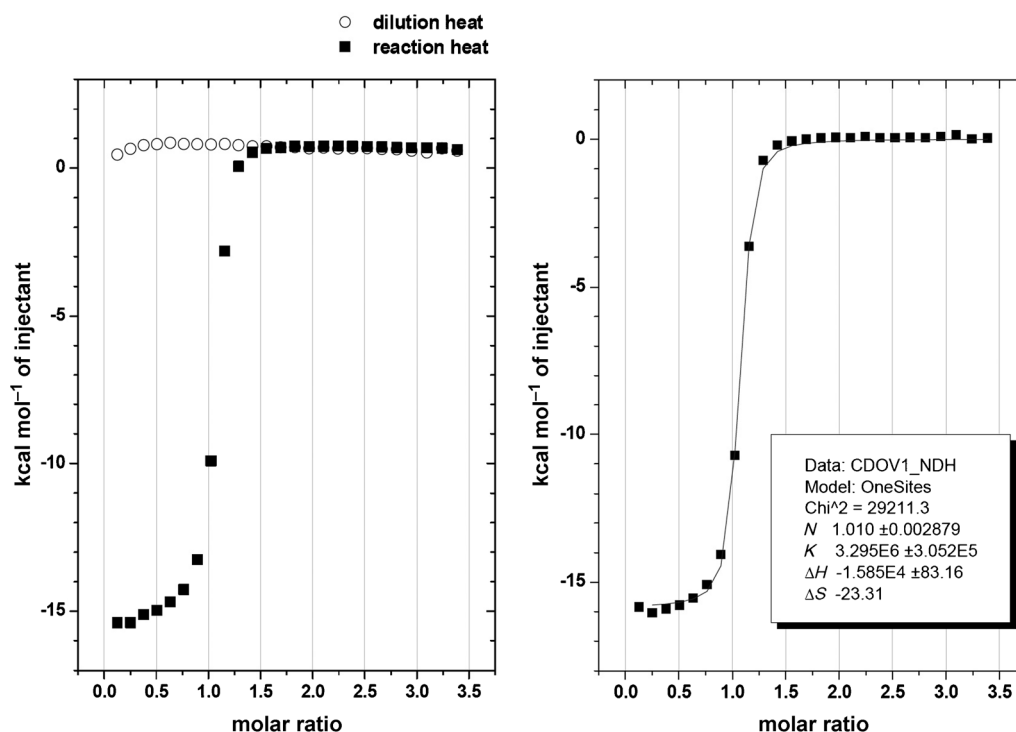


Figure 10. a) Heat effects of complexation and of dilution of **1** with **2** for each injection during titration microcalorimetric experiment; b) the "net" heat-effect obtained by subtracting the heat of dilution from the heat of reaction, which was analyzed by computer simulation using the "one set of binding sites" model.

Table 1. Stability constant (K_S) and enthalpy (ΔH) for **1** with **2**, **1·2** with CB[8], and **2** with CB[8] in aqueous phosphate buffer solutions of pH 7.2 at 298 K.

Complexation reaction	K_S	$-\Delta H$ [kJ mol ⁻¹]
$1+2=1\cdot2$ ^[a]	$(3.3\pm0.3)\times10^6\text{ M}^{-1}$	66.0 ± 0.5
$2+\text{CB}[8]=2\cdot\text{CB}[8]$	$(1.4\pm0.3)\times10^5\text{ M}^{-1}$ ^[c]	24.6 ± 0.1 ^[e]
$1+2+\text{CB}[8]=1\cdot2\cdot\text{CB}[8]$	$(7.4\pm0.5)\times10^9\text{ M}^{-2}$ ^[b]	—
$2+\alpha\text{-CD}=2\cdot\alpha\text{-CD}$ ^[d]	$(2360\pm24)\text{ M}^{-1}$	22.3 ± 0.1
$2\cdot\text{CB}[8]+3=2\cdot3\cdot\text{CB}[8]$	—	—
$2+\text{CB}[8]+3=2\cdot3\cdot\text{CB}[8]$	$10^{11}\text{ to }10^{13}\text{ M}^{-2}$	—

[a] Measured directly by ITC; the net reaction heat in this run was calculated by the “one set of binding sites” model in ORIGIN software ([Host **1**] 10.0–20.0 mM, [Guest **2**] 0.5–1.0 mM). [b] Measured directly by ¹H NMR integration of free and bound guest. [c] Measured directly by UV/Vis spectrum. [d] See ref. [25]. [e] Values corresponding to the model of single one-site–one-site interaction.

mation, Figures S28 and S29) is nearly two orders of magnitude larger than that of α -CD and **2** and relatively smaller than that of the complex **1·2**. When CB[8] was added into the solution of the complex **1·2**, the more stable 1:1:1 ternary complex **1·2·CB[8]** is formed and the binding constant is $7.4\times10^9\text{ M}^{-2}$, which is much larger than those of individual two-component complexes (see the Supporting Information, Figure S30 and Table S1). This information indicates that the formation of ternary complexes between **1**, **2**, and CB[8] have a priority over that of the two-component complexes in aqueous solutions.

A K_S value for the ternary complex **2·3·CB[8]** of up to 10^{11} M^{-2} was obtained, which is about two orders of magnitude larger than ternary complex **1·2·CB[8]**. Thus, in this four-component system, CB[8] moves from the ternary system of **1·2·CB[8]** and encapsulates the bipyridium of **2** and **3** (leading to the formation of the most stable 1:1:1 ternary complex) and subsequently, the octyl chains insert spontaneously into the α -CD cavity of **1** from the secondary face, ultimately resulting in the formation of the heterowheel polypseudorotaxane. All these results reveal that the processes are thermodynamically controlled. Such selective social self-sorting processes in aqueous is unusual based on the different recognition behavior of cyclodextrins and cucurbiturils.

TEM, AFM, DLS, DOSY, and viscosity measurements:

Both transmission electron microscopic (TEM) and atomic force microscopic (AFM) experiments were performed to give the visual information about the size and shape of the heterowheel polypseudorotaxane **1·2·3·CB[8]**. As shown in Figure 11a, several parallel fiber-like linear assemblies were observed on the substrate. Their length is more than 100 nm. Furthermore, the AFM image (Figure 11b) shows the fine structure of the linear assemblies with the height from 1.5 to 5 nm, which is larger than the diameter of α -CD (1.5 nm). This is attributed to the aggregation process through the intermolecular hydrogen bonding between –OH groups on the secondary face parallel to each other,^[27] which is consistent with the result of the TEM experiments.

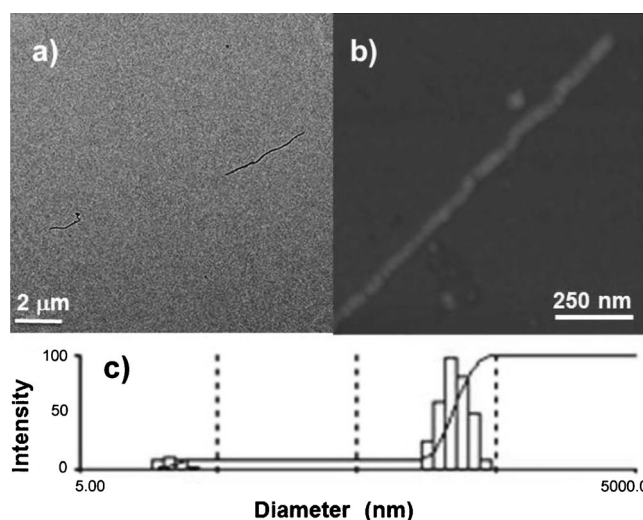


Figure 11. a) TEM image (0.50 μm) and b) AFM image of the heterowheel polypseudorotaxane from equimolar four components; c) Distribution of the hydrodynamic diameter of the heterowheel polypseudorotaxane (0.50 μm) in aqueous solution at 298 K.

Dynamic-light scattering (DLS) was used for measuring the size distribution of the aggregates in aqueous solution. The results obtained show that the size distribution of the assemblies falls into two categories: one from 1.8 to 3.3 nm should belong to the monomer of **1** and the other broad peak from 90 to 380 nm belongs to a variety of highly linear supramolecular assemblies with an average diameter of 226 nm (Figure 11c). The assembly sizes measured by DLS are not in accordance with those observed on TEM images, because TEM was performed under a dry state but DLS measures the solvated particle size in aqueous solution. Diffusion-ordered spectroscopy (DOSY) experiments were also performed to investigate the self-sorting process among the four components. As can be seen from Figures S31 to S33 in the Supporting Information, the measured weight average diffusion coefficients were decreased considerably from 2.65×10^{-10} (**2·CB[8]**), 2.38×10^{-10} (**2·3·CB[8]**) to $1.67\times10^{-10}\text{ m}^2\text{ s}^{-1}$ (**1·2·3·CB[8]**). This result indicates an increase in the average aggregation size owing to aggregation process through the four components.

Additionally, viscosity measurements provided further evidence for the formation of heterowheel polypseudorotaxane, in which viscosity transitions represent a critical aggregation concentration from the formation of monomers or oligomers to highly ordered supramolecular polymers.^[28] As shown in the logarithmic plot of specific viscosity versus concentration of assembly **1·2·3·CB[8]** (Figure S34 in the Supporting Information), a gradual increase for the predominance of the resulting assembly was observed with its concentrations, accompanied with the appearance of a clear inflection point at $8.35\times10^{-5}\text{ M}$. These results obtained further support the supramolecular polymerization process of **1**, **2**, **3** and CB[8] in water.

Conclusion

We selected two macrocycles and two plain organic molecules as the self-sorting components to fabricate a heterowheel polypseudorotaxane. Six complexes were obtained by mixing two or three of the four organic molecules, but the addition of the other one or two components exclusively led to the formation of the thermodynamically stable supramolecular heterowheel polypseudorotaxane. Hydrophobic-, ion-dipole-, and charge-transfer interactions are the driving forces for the interpenetration of axle molecules into the cavity of wheel components to form polypseudorotaxanes. To the best of our knowledge, the heterowheel polypseudorotaxane is the first artificial fully organic four-component social self-sorting system. The current study could open new doors for the investigation of social self-sorting systems in biological processes.

Acknowledgements

This work was supported by the 973 Program (2011CB932500), NNSFC (Nos.: 20932004 and 20972077).

- [1] In a multicomponent system, if a molecule shows higher affinity for one of components of complex, and another molecule binds more tightly to the other in the same complex, only two complexes are formed almost independent from the stoichiometry of the components, which is usually considered as social self-sorting; see: a) A. Wu, L. Isaacs, *J. Am. Chem. Soc.* **2003**, *125*, 4831–4835; b) S. Liu, C. Ruspici, P. Mukhopadhyay, S. Chakrabarti, P. Y. Zavalij, L. Isaacs, *J. Am. Chem. Soc.* **2005**, *127*, 15959–15967; c) P. Mukhopadhyay, A. Wu, L. Isaacs, *J. Org. Chem.* **2004**, *69*, 6157–6164; d) A. Wu, L. Isaacs, *J. Am. Chem. Soc.* **2003**, *125*, 4831–4835; e) S. Ghosh, A. Wu, J. C. Fetting, P. Y. Zavalij, L. Isaacs, *J. Org. Chem.* **2008**, *73*, 5915–5925; f) A. Wu, A. Chakraborty, J. C. Fetting, R. A. Flowers II, L. Isaacs, *Angew. Chem.* **2002**, *114*, 4200–4203; *Angew. Chem. Int. Ed.* **2002**, *41*, 4028–4031; g) C. Burd, M. Weck, *Macromolecules* **2005**, *38*, 7225–7230; h) H.-J. Schneider, A. K. Yatsimirsky, *Chem. Soc. Rev.* **2008**, *37*, 263–277; i) M. M. Safont-Sempere, G. Fernandez, F. Wurthner, *Chem. Rev.* **2011**, *111*, 5784–5814; j) W. Jiang, Q. Wang, I. Linder, F. Klautzsch, C. A. Schalley, *Chem. Eur. J.* **2011**, *17*, 2344–2348.
- [2] a) M. R. Molla, A. Das, S. Ghosh, *Chem. Eur. J.* **2010**, *16*, 10084–10093; b) K. A. Jolliffe, P. Timmerman, D. N. Reinhoudt, *Angew. Chem.* **1999**, *111*, 983–986; *Angew. Chem. Int. Ed.* **1999**, *38*, 933–937; c) C. Burd, M. Weck, *Macromolecules* **2005**, *38*, 7225–7230; d) S. Xu, N. Giuseppone, *J. Am. Chem. Soc.* **2008**, *130*, 1826–1827; e) D. Braekers, C. Peters, A. Bogdan, Y. Rudzevich, V. Böhmer, J. F. Desreux, *J. Org. Chem.* **2008**, *73*, 701–706; f) D. Ajami, J.-L. Hou, T. J. Dale, E. Barrett, J. Rebek, Jr., *Proc. Natl. Acad. Sci. USA* **2009**, *106*, 10430–10434; g) E. S. Barrett, T. J. Dale, J. Rebek, Jr., *J. Am. Chem. Soc.* **2008**, *130*, 2344–2350; h) N.-T. Lin, A. V. Jentzsch, L. Guénée, J.-M. Neudörfl, S. Aziz, A. Berkessel, E. Orentas, N. Sakai, S. Matile, *Chem. Sci.* **2012**, *3*, 1121–1127.
- [3] a) J. R. Nitschke, J.-M. Lehn, *Proc. Natl. Acad. Sci. USA* **2003**, *100*, 11970–11974; b) S. Ulrich, J.-M. Lehn, *J. Am. Chem. Soc.* **2009**, *131*, 5546–5559.
- [4] a) W. S. Jeon, K. Moon, S. H. Park, H. Chun, Y. H. Ko, J. Y. Lee, E. S. Lee, S. Samal, N. Selvapalam, M. V. Rekharsky, V. Sindelar, D. Sobransingh, Y. Inoue, A. E. Kaifer, K. Kim, *J. Am. Chem. Soc.* **2005**, *127*, 12984–12989; b) S. J. Rowan, D. G. Hamilton, P. A. Brady, J. K. M. Sanders, *J. Am. Chem. Soc.* **1997**, *119*, 2578–2579; c) J.-B. Lin, X.-N. Xu, X.-K. Jiang, Z.-T. Li, *J. Org. Chem.* **2008**, *73*, 9403–9410; d) H. Gan, B. C. Gibb, *Chem. Commun.* **2012**, *48*, 1656–1658.
- [5] N. Tomimatsu, A. Kanaya, Y. Takashima, H. Yamaguchi, A. Harada, *J. Am. Chem. Soc.* **2009**, *131*, 12339–12343.
- [6] a) F. Wang, B. Zheng, K. Zhu, Q. Zhou, C. Zhai, S. Li, N. Li, F. Huang, *Chem. Commun.* **2009**, 4375–4377; b) S. Dong, X. Yan, B. Zheng, J. Chen, X. Ding, Y. Yu, D. Xu, M. Zhang, F. Huang, *Chem. Eur. J.* **2012**, *18*, 4195–4199.
- [7] a) W. Jiang, C. A. Schalley, *J. Mass Spectrom.* **2010**, *45*, 788–798; b) W. Jiang, H. D. F. Winkler, C. A. Schalley, *J. Am. Chem. Soc.* **2008**, *130*, 13852–13853; c) W. Jiang, C. A. Schalley, *Proc. Natl. Acad. Sci. USA* **2009**, *106*, 10425–10429; d) G. Celtek, M. Artar, O. A. Scherman, D. Tuncel, *Chem. Eur. J.* **2009**, *15*, 10360–10363; e) E. Masson, X. Lu, X. Ling, D. L. Patchell, *Org. Lett.* **2009**, *11*, 3798–3801; f) A. S. Singh, S.-S. Sun, *Chem. Commun.* **2012**, *48*, 7392–7394.
- [8] a) S. J. Lee, S.-H. Cho, K. L. Mulfort, D. M. Tiede, J. T. Hupp, S. T. Nguyen, *J. Am. Chem. Soc.* **2008**, *130*, 16828–16829; b) B. H. Northrop, Y.-R. Zheng, K.-W. Chi, P. J. Stang, *Acc. Chem. Res.* **2009**, *42*, 1554–1563; c) S. R. Seidel, P. J. Stang, *Acc. Chem. Res.* **2002**, *35*, 972–983.
- [9] a) A.-M. L. Fuller, D. A. Leigh, P. J. Lusby, *J. Am. Chem. Soc.* **2010**, *132*, 4954–4959; b) C. Talotta, C. Gaeta, T. Pierro, P. Neri, *Org. Lett.* **2011**, *13*, 2098–2101.
- [10] a) A. Carlone, S. M. Goldup, N. Lebrasseur, D. A. Leigh, A. Wilson, *J. Am. Chem. Soc.* **2012**, *134*, 8321–8323; b) H. M. Cheng, D. A. Leigh, F. Maffei, P. R. McGonigal, A. M. Z. Slawin, J. Wu, *J. Am. Chem. Soc.* **2011**, *133*, 12298–12303; c) J.-F. Ayme, J. E. Beves, D. A. Leigh, R. T. McBurney, K. Rissanen, D. Schultz, *J. Am. Chem. Soc.* **2012**, *134*, 9488–9497; d) P. E. Barran, H. L. Cole, S. M. Goldup, D. A. Leigh, P. R. McGonigal, M. D. Symes, J. Wu, M. Zengerle, *Angew. Chem.* **2011**, *123*, 12488–12492; *Angew. Chem. Int. Ed.* **2011**, *50*, 12280–12284.
- [11] a) R. A. Bilbeisi, J. K. Clegg, N. Elgrishi, X. de Hatten, M. Devillard, B. Breiner, P. Mal, J. R. Nitschke, *J. Am. Chem. Soc.* **2012**, *134*, 5110–5119; b) P. Mal, D. Schultz, K. Beyeh, K. Rissanen, J. R. Nitschke, *Angew. Chem.* **2008**, *120*, 8421–8425; *Angew. Chem. Int. Ed.* **2008**, *47*, 8297–8301; c) R. J. Sarma, J. R. Nitschke, *Angew. Chem.* **2008**, *120*, 383–386; *Angew. Chem. Int. Ed.* **2008**, *47*, 377–380.
- [12] a) K. Mahata, M. L. Saha, M. Schmittel, *J. Am. Chem. Soc.* **2010**, *132*, 15933–15935; b) K. Mahata, M. Schmittel, *J. Am. Chem. Soc.* **2009**, *131*, 16544–16554; c) M. Schmittel, K. Mahata, *Chem. Commun.* **2010**, *46*, 4163–4165; d) M. M. J. Smulders, A. Jimenez, J. R. Nitschke, *Angew. Chem.* **2012**, *124*, 6785–6789; *Angew. Chem. Int. Ed.* **2012**, *51*, 6681–6685.
- [13] a) Y. Liu, Y. Chen, *Acc. Chem. Res.* **2006**, *39*, 681–691; b) Y. Liu, Z.-X. Yang, Y. Chen, Y. Song, N. Shao, *ACS Nano* **2008**, *2*, 554–560; c) Y.-L. Zhao, H.-Y. Zhang, M. Wang, H.-M. Yu, H. Yang, Y. Liu, *J. Org. Chem.* **2006**, *71*, 6010–6019; d) Y. Chen, Y. Liu, *Chem. Soc. Rev.* **2010**, *39*, 495–505; e) A. Harada, Y. Takashima, H. Yamaguchi, *Chem. Soc. Rev.* **2009**, *38*, 875–882; f) M. V. Rekharsky, Y. Inoue, *Chem. Rev.* **1998**, *98*, 1875–1917.
- [14] a) K. Johnstone, N. Bampos, M. J. Gunter, J. K. M. Sanders, *Chem. Commun.* **2003**, 1396–1397; b) G. Kaiser, T. Jarrosson, S. Otto, Y.-F. Ng, J. K. M. Sanders, *Angew. Chem.* **2004**, *116*, 1993–1996; *Angew. Chem. Int. Ed.* **2004**, *43*, 1959–1962; c) S. A. Vignon, T. Jarrosson, T. Iijima, H.-R. Tseng, J. K. M. Sanders, J. F. Stoddart, *J. Am. Chem. Soc.* **2004**, *126*, 9884–9885; d) T. Iijima, S. A. Vignon, H.-R. Tseng, T. Jarrosson, J. K. M. Sanders, F. Marchioni, M. Venturi, E. Apostoli, V. Balzani, J. F. Stoddart, *Chem. Eur. J.* **2004**, *10*, 6375–6392.
- [15] a) J. Lagona, P. Mukhopadhyay, S. Chakrabarti, L. Isaacs, *Angew. Chem.* **2005**, *117*, 4922–4949; *Angew. Chem. Int. Ed.* **2005**, *44*, 4844–4870; b) Y. H. Ko, E. Kim, I. Hwang, K. Kim, *Chem. Commun.* **2007**, 1305–1312.
- [16] a) U. Rauwald, O. A. Scherman, *Angew. Chem.* **2008**, *120*, 4014–4017; *Angew. Chem. Int. Ed.* **2008**, *47*, 3950–3953; b) S. Deroo, U. Rauwald, C. V. Robinson, O. A. Scherman, *Chem. Commun.* **2009**,

- 6, 644–646; c) J. M. Zayed, F. Biedermann, U. Rauwald, O. A. Scherman, *Polym. Chem.* **2010**, *1*, 1434–1436.
- [17] F. Tian, N. Cheng, N. Nouvel, J. Geng, O. A. Scherman, *Langmuir* **2010**, *26*, 5323–5328.
- [18] a) E. A. Appel, F. Biedermann, U. Rauwald, S. T. Jones, J. M. Zayed, O. A. Scherman, *J. Am. Chem. Soc.* **2010**, *132*, 14251–14260; b) R. J. Coulston, S. T. Jones, T. C. Lee, E. A. Appel, O. A. Scherman, *Chem. Commun.* **2011**, *47*, 164–166.
- [19] F. Biedermann, U. Rauwald, J. M. Zayed, O. A. Scherman, *Chem. Sci.* **2011**, *2*, 279–286.
- [20] Z.-J. Ding, H.-Y. Zhang, L.-H. Wang, F. Ding, Y. Liu, *Org. Lett.* **2011**, *13*, 856–859.
- [21] a) Y. Liu, C.-F. Ke, H.-Y. Zhang, W.-J. Wu, J. Shi, *J. Org. Chem.* **2007**, *72*, 280–283; b) C.-F. Ke, S. Hou, H.-Y. Zhang, Y. Liu, K. Yang, X.-Z. Feng, *Chem. Commun.* **2007**, 3374–3376; c) C. Ke, R. A. Smaldone, T. Kikuchi, H. Li, A. P. Davis, J. F. Stoddart, *Angew. Chem.* **2013**, *125*, 399–405; *Angew. Chem. Int. Ed.* **2013**, *52*, 381–387.
- [22] a) Y. Liu, C.-F. Ke, H.-Y. Zhang, J. Cui, F. Ding, *J. Am. Chem. Soc.* **2008**, *130*, 600–605; b) L. Li, C. F. Ke, H.-Y. Zhang, Y. Liu, *J. Org. Chem.* **2010**, *75*, 6673–6676.
- [23] M. Kajtár, C. Horvath-Toro, E. Kuthi, J. Szejtli, *Acta Chim. Acad. Sci. Hung.* **1982**, *110*, 327–355.
- [24] a) H.-J. Kim, J. Heo, W. S. Jeon, E. Lee, J. Kim, S. Sakamoto, K. Yamaguchi, K. Kim, *Angew. Chem.* **2001**, *113*, 1574–1577; *Angew. Chem. Int. Ed.* **2001**, *40*, 1526–1529; b) A. Trabolsi, M. Hmadeh, N. M. Khashab, D. C. Friedman, M. E. Belowich, N. Humbert, M. Elhabiri, H. Khatib, A. A.-M. Albrecht-Gary, J. F. Stoddart, *New J. Chem.* **2009**, *33*, 254–263.
- [25] Y. Liu, X.-Y. Li, H.-Y. Zhang, C.-J. Li, F. Ding, *J. Org. Chem.* **2007**, *72*, 3640–3645.
- [26] M. V. Rekharsky, Y. Inoue, *Chem. Rev.* **1998**, *98*, 1875–1918.
- [27] S. S. Jaffer, S. K. Saha, G. Eranna, A. K. Sharma, P. Purkayastha, *J. Phys. Chem. C* **2008**, *112*, 11199–11204.
- [28] S. Dong, Y. Luo, X. Yan, B. Zheng, X. Ding, Y. Yu, Z. Ma, Q. Zhao, F. Huang, *Angew. Chem.* **2011**, *123*, 1945–1949; *Angew. Chem. Int. Ed.* **2011**, *50*, 1905–1909.

Received: December 25, 2012

Revised: February 15, 2013

Published online: March 15, 2013